Kinetic Implications of Nonlinear Effects in Asymmetric Synthesis

Donna G. Blackmond

Contribution from the Max-Planck-Institut für Kohlenforschung, Kaiser Wilhelm Platz 1, Mülheim an der Ruhr, D-45470 Germany

Received July 13, 1998

Abstract: Observation of a conversion-dependent enantioselectivity in asymmetric reactions with nonenantiopure catalysts or reagents may be diagnostic of kinetically complex behavior. This paper shows how reaction simulations based on parameters derived from initial enantioselectivity data provide an extension of the Kagan ML_n models as powerful mechanistic tools in asymmetric synthesis. This approach is illustrated for an example of a stoichiometric reduction of aralkyl ketones with chiral borane reagents and is also discussed for several cases of catalytic reactions.

Introduction

It has been known for some time that mixtures of enantiomers sometimes exhibit unusual physical and chemical properties attributable to the formation of diastereomeric species in solutions.[1] For example, the NMR spectrum of a racemic mixture of enantiomeric compounds may differ from that of the pure enantiomer,[2] or the rate of an organic reaction involving a racemic mixture of chiral compounds may be different from that using the corresponding enantiomerically pure compound.[3] When the enantiomeric excess obtained in the products of an asymmetric reaction is not linearly proportional to the optical purity of the chiral catalyst or chiral auxiliary used, this has been termed either a positive ("asymmetric amplification") or a negative nonlinear effect, depending on the direction of deviation from the enantioselectivity expected when an enantiopure catalyst or auxiliary is used. Kagan and co-workers[4,5] first described nonlinear effects of the enantiopurity of a catalyst or chiral auxiliary on the product enantiomeric excess in asymmetric reactions, and they developed mathematical models of this behavior which help elucidate mechanistic information about the reaction. Numerous other catalytic and stoichiometric examples of these nonlinear effects have since been reported,[6] and analysis in terms of Kagan's models has proved to be a powerful diagnostic tool in many cases.

The discussion of nonlinear effects of catalyst or auxiliary enantiopurity has to date focused primarily on the nature of the chiral species and on how these species form and interact in and outside the reaction cycle, and structural and spectroscopic studies aimed at a stereochemical rationalization of the observed nonlinear phenomena outnumber kinetic approaches toward mechanistic understanding. We recently reported an extension of Kagan's models to include consideration of the reaction rate, demonstrating how this information may help to support or reject proposed reaction mechanisms as well as to provide insight for practical synthetic strategies employing nonenantiopure catalysts.[7,8] A further kinetic complication which was not treated in that work is a dependence of enantioselectivity on reaction time or substrate conversion, which has been noted in a number of experimental studies.[6c,h,i] The mechanistic implications which derive from such a conversion-dependent enantioselectivity in asymmetric reactions using nonenantiopure reagents and a protocol for the general use of Kagan's models in cases such as this are discussed in this paper. This diagnostic tool is demonstrated for the case of a stoichiometric asymmetric reaction reported by workers at Merck,[9] and comments about an extension to catalytic systems follow this discussion.

Results and Discussion

Modeling and Reaction Simulation Based on Initial Enantioselectivity Data. A temporal enantioselectivity dependence

(1) (a) Horeau, A. *Tetrahedron Lett*. **1969**, 3121−3124. (b) Horeau, A.; Guetté, J. P. *Tetrahedron* **1974**, *30*, 1923−1931.

(2) (a) Williams, T.; Pitcher, R. G.; Gutzwiller, J.; Uskovic, M. *J. Am. Chem. Soc*. **1969**, *91*, 1871−1872. (b) Harger, M. J. P. *Chem. Commun*. **1976**, 555−556. (c) Kabachnik, MI.; Mastrywkova, T. A.; Fedin, E. I.; Vaisberg, M. S.; Morozov, L. I.; Petrovsky, P. V.; Shipov, A. E. *Tetrahedron* **1976**, *32*, 1719−1728.

(3) Wynberg, H.; Feringa, B. L.; *Tetrahedron* **1976**, *32*, 2831−2834.

(4) (a) Guillaneux, D.; Zhao, S. H.; Samuel, O.; Rainford, D.; Kagan, H. B.; *J. Am. Chem. Soc*. **1994**, *116*, 9430−39. (b) Puchot, C.; Samuel, O.; Duñach, E.; Zhao, S.; Agami, C.; Kagan, H. B. *J. Am. Chem. Soc*. **1986**, *108*, 2353−57.

(5) For recent reviews see: (a) Kagan, H. B. *Angew. Chem.* In press. (b) Kagan, H. B.; Girard, C.; Guillaneux, D.; Rainford, D.; Samuel, O.; Zhang, S. Y.; Zhao, S. H. *Acta Chem. Scand*. **1996**, *30*, 345−352. (c) Bolm, C. In *Advanced Asymmetric Synthesis*; Stephenson, G. R., Ed.; Blackie A&P: Glasgow, 1996; pp 9−26. (d) Avalos, M.; Babiano, R.; Cintas, P.; Jiménez, J. L.; Palacios, J. C. *Tetrahedron Asymm*. **1997**, *8*, 2997−3017.

(6) (a) Oguni, N.; Matsuda, Y.; Kaneko, T. *J. Am. Chem. Soc*. **1988**, *110*, 7877. (b) Noyori, R.; Kitamura, M. *Angew. Chem., Int. Ed. Engl*. **1991**, *30*, 49. (c) Bolm, C.; Ewald, M.; Fleder, M. *Chem. Ber*. **1992**, *125*, 1205. (d) Mikami, K.; Matsukawa T. *Tetrahedron* **1992**, *48*, 5671. (e) Rossiter, B. E.; Miao, G.; Swingle, N. M.; Eguchi, M.; Hernández, A. E.; Patterson, R. G. *Tetrahedron Asymm*. **1992**, *3*, 231. (f) Keck, G. E.; Krishnamurthy, D.; Grier, M. C. *J. Org. Chem*. **1993**, *58*, 6543. (g) Evans, D. E.; Nelson, S. G.; Gagné, M.; Muci, A. R. *J. Am. Chem. Soc*. **1993**, *115*, 9800. (h) Komatsu, N.; Hashizume, M.; Sugita, T.; Uemura, S. *J. Org. Chem*. **1993**, *58*, 4529. (i) de Vries, A. H. M.; Jansen, J. F. G. A.; Feringa, B. L. *Tetrahedron* **1994**, *50*, 4479. (j) Zhou, Q.-L.; Pfaltz, A. *Tetrahedron* **1994**, *50*, 4467. (k) Kitamura, M.; Suga, S.; Niwa, M.; Noyori, R. *J. Am. Chem. Soc*. **1995**, *117*, 4832. (l) Keck, G. E.; Krishnamurthy, D. *J. Am. Chem. Soc*. **1995**, *117*, 2363. (m) Bougauchi, M.; Watanabe, S.; Arai, T.; Sasai, H.; Shibasaki, M. *J. Am. Chem. Soc*. **1997**, *119*, 2329.

(7) Blackmond, D. G. *J. Am. Chem. Soc*. **1997**, *119*, 12934.

(8) In the nucleophilic addition of dialkylzinc to aldehydes with chiral amino alcohols, Oguni (ref 6a) briefly noted effects on reaction rate in accordance with those described in ref 7, and Noyori (ref 6k) has studied nonlinear effects on reaction rate.

(9) (a) Shinkai, I.; King, A. O.; Larsen, R. D. *Pure Appl. Chem*. **1994**, *66*, 1551. (b) King, A. O.; Corley, E. G.; Anderson, R. K.; Larsen, R. D.; Verhoeven, T. R.; Reider, P. J.; Xiang, Y. B.; Belley, M.; Leblanc, Y.; Labelle, M.; Prasit, P.; Zamboni, R. J. *J. Org. Chem*. **1993**, *58*, 3731−3735. (c) Zhao, M.; King, A. O.; Larsen, R. D.; Verhoeven, T. R.; Reider, R. J. *Tetrahedron Lett*. **1997**, *38*, 2641−2644.

10.1021/ja982448u CCC: $15.00
Published on Web 12/03/1998

Scheme 1

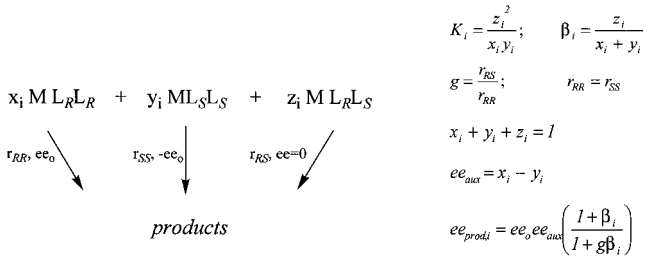

may arise for a number of reasons which violate one or more of the tenets on which the ML_n models are based. These include (a) fast ligand exchange (dynamic equilibrium) between the chiral species present in the reaction mixture, (b) identical reaction rate laws followed by each chiral species present, and (c) absence of reaction-driven phenomena such as product inhibition or autocatalysis. In the limit of very low conversion, it may be argued that each of these assumptions will hold even in cases where it clearly breaks down as the reaction progresses. Applying an ML_2 model fit[4] to *initial* enantioselectivity data $ee_{prod,i}$ thus provides a means of determining the relative *initial* concentrations of the chiral species (Scheme 1, where x_i, y_i, and z_i refer to the initial relative concentrations of the enantiopure and *meso* species). Even for cases where the chiral auxiliary or catalyst changes over time, knowledge of its initial condition is important for tracing its fate over the course of the reaction, which may be investigated through kinetic modeling of the reaction based on these initial conditions. The parameters *K* and *g* (respectively describing the relative initial abundance and reactivity of the *meso* species in an ML_2 model) derived from the model fit to the initial ee data may thus be used in a mathematical simulation of the reaction to predict the conversion dependence of the product enantioselectivity. The form of the expressions describing the reaction rates and concentrations of each species as a function of time which are to be used in the simulations will be based on mechanistic proposals for the particular system under study concerning the origin of the conversion dependence. If the predictions from such a simulation are borne out by the experimental data, this would lend strong support to the proposed reaction mechanism, since it provides an independent test of the experimental reaction results.

Example: Stoichiometric Reduction of Aralkyl Ketones with Dimeric Chiral Borane Reagents. The practical exploitation of the phenomenon of nonlinear effects was recently realized in pharmaceutical production by scientists at Merck in the preparation of an LTD_4 antagonist for the treatment of asthma.[9] They developed an in-situ preparation of diisopinocampheylchloroborane (Ipc_2BCl), a chiral borane compound originally introduced by Brown[10] for the stoichiometric reduction of aralkyl ketones (eq 1).

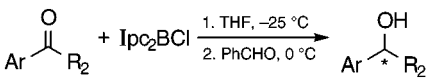

(1)

Although the enantiopurity of the reagent was not measured, the Merck workers found that the use of Ipc_2BCl prepared from 85% ee α-pinene was as effective in producing highly enantiopure alcohols as was the reagent prepared from the more expensive 97% ee starting material. Brown and co-workers had previously recognized that the enantiopurity of diisopinocampheylborane (Ipc_2BH)[10d] and Ipc_2BCl could exceed that of the starting material when an exess of α-pinene was used in preparation of the dimeric chiral reagent. They suggested that reductions carried out with enantiopure reagents prepared in this way may also serve as a convenient method for obtaining optically pure α-pinene, which is liberated during the reaction.

Scheme 2

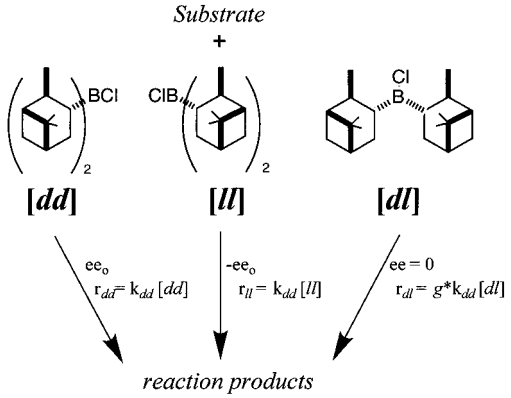

The asymmetric amplification noted in the reactions carried out in the Merck studies was accompanied by a conversion-dependent enantioselectivity, and both were especially pronounced for reactions using the Ipc_2BCl reagent prepared with α-pinene of lower enantiopurities.[9c] A plot of final product enantioselectivity vs the enantiomeric excess of the chiral borane reagent came close to that predicted from Kagan's ML_2 model (Scheme 2) for a statistical distribution ($K = 4$) of active homochiral and inactive ($g = 0$) *meso* complexes. That this apparent agreement between the experimental values and the model fit must be purely coincidental was also noted by these authors, since changes in enantioselectivity with reaction progress cannot be accounted for in the ML_n models. Kagan and co-workers[5b,11] have noted that for a stoichiometric reaction with nonenantiopure reagents, the relative concentrations of the chiral auxiliary species change over the course of the reaction when the homo- and heterochiral species are consumed at different rates. Thus the assumption of dynamic equilibrium between the chiral species does not hold in this case. Kagan also pointed out,[5b] however, that this assumption will hold approximately when a very large excess of chiral auxiliary is employed. Similarly, it may be noted that the relative concentrations of the chiral reagents may be treated as constant in the limit of very low conversion, regardless of the amount of the chiral reagent employed.

The Merck study of ref 9c thus provides a case where the kinetic modeling approach outlined above may be applied. Figure 1a shows the initial enantioselectivity experimental data points up to $ee_{aux} = 0.7$ reproduced from ref 9c. The solid line shows the ML_2 model fit to those experimental data that was performed in the present work, and which affords an excellent fit with parameters $K = 49$ and $g = 0.1$. These parameters provide important mechanistic information about the reaction. The model value of $g = 0.1$ shows that the *meso* complex was not completely inactive, as indeed the conversion dependence of the product enantioselectivity also implied. The large value of *K* indicates that the system did indeed form a nonrandom mixture of chiral species, exhibiting a larger fraction of *meso* species than would be expected from the statistical distribution.

(10) (a) Brown, H. C.; Chandrasekharan, J.; Ramachandran, P. V. *J. Org. Chem.* **1985**, *50*, 5446. (b) Brown, H. C.; Srebnik, M.; Ramachandran, P. V. *J. Org. Chem.* **1989**, *54*, 1577. (c) Brown, H. C.; Chandrasekharan, J.; Ramachandran, P. V. *J. Am. Chem. Soc.* **1988**, *110*, 1539. (d) Brown, H. C.; Desai, M. C.; Jadhav, P. K. *J. Org. Chem.* **1982**, *47*, 5065.

(11) (a) Girard, C.; Kagan, H. B. *Tetrahedron Asymm.* **1995**, *6*, 1881−1884. (b) Girard, C.; Kagan, H. B. *Tetrahedron Asymm.* **1997**, *8*, 3851−3854.

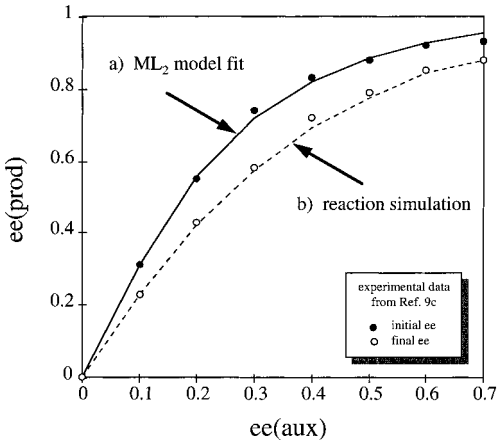

Figure 1. Experimental (ref 3c) and modeling (this work) results of nonlinear behavior in the stoichiometric asymmetric reduction of aralkyl ketones with use of 1 equiv of Ipc_2BCl prepared from α-pinene of different enantiopurities (see eq 1 and Scheme 1): ●, experimental data for initial product enantioselectivity from ref 9c; ○, experimental data for final product enantioselectivity from ref 9c. (a) ML_2 model fit to the experimental initial product ee data, giving $K = 49$ and $g = 0.1$ (—). (b) Simulation of the reaction to the expeimental reaction endpoint to give final product enantioselectivity data (---).

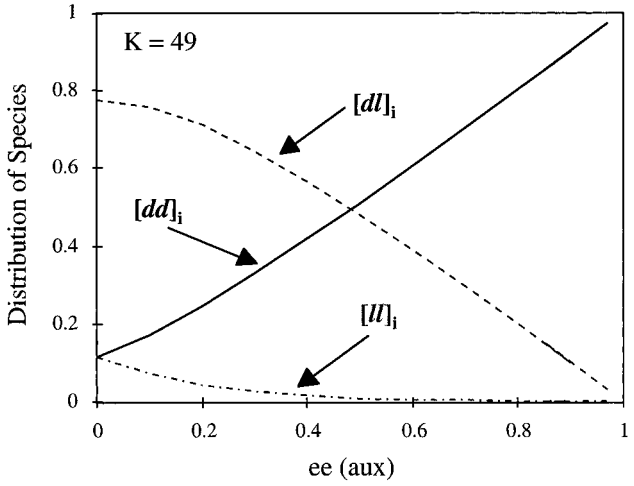

Figure 2. Initial distribution of species $[dd]_i$, $[ll]_i$, and $[dl]_i$ as a function of ee_{aux} for the value of $K = 49$ predicted by the ML_2 model fit to the initial enantioselectivity data shown in Figure 1a.

For example, a racemic mixture in this case contains only 11% of each pure species and 78% of the *meso* species, compared to 25% pure and 50% *meso* for the case of a racemic statistical distribution ($K = 4$). Figure 2 shows the relationship between the initial distribution of species $[dd]_i$, $[ll]_i$, and $[dl]_i$ and ee_{aux}, calculated from the model fit to the initial enantioselectivity data as described in ref 7.

The starting conditions fixed by this ML_2 model fit to the initial enantioselectivity data were then used to carry out separate simulations of the reactions of mixtures of the three chiral species values from 0 to 0.7. The simulation adheres to all of the assumptions of the ML_2 model except that the *dd*, *ll*, and *dl* species are consumed at the relative rates prescribed by the parameters found in the model fit to the initial ee data. Thus the *dd* and *ll* species react with the identical rate constant k_{dd} and produce reaction products with opposite enantioselectivity ee_o and $-ee_o$. The *dl* species is one-tenth as active as the enantiopure complexes ($k_{dl} = g*k_{dd}$, g = 0.1) and produces racemic product (ee = 0). With these conditions, it may be shown that the cumulative product enantioselectivity at any instant in time will be described by eq 2:

$$ee_{prod,f}(t) = \frac{\sum R - \sum S}{\sum R + \sum S} = \frac{ee_o([dd]_i - [ll]_i)(1 - \exp(-k_{dd}t))}{([dd]_i + [ll]_i)(1 - \exp(-k_{dd}t)) + [dl]_i(1 - \exp(-gk_{dd}t))} \quad (2)$$

This equation shows that, as noted by Kagan and co-workers,[5b] it is only when the *meso* species is completely inactive ($g = 0$) that no change in product enantioselectivity with conversion will be observed in a stoichiometric reaction of nonenantiopure reagents.

The results of the reaction simulations using eq 2 are shown as the dotted line in Figure 1b. This curve for $ee_{prod,f}$ differs from the solid line shown for the initial ee data in an important way: it is *not* a fit to the data points, but it is instead a set of six separate predictions[12] which are independent of the experimentally found values for the final product enantioselectivities, and are based only on the parameters ($[dd]_i$, $[ll]_i$, $[dl]_i$, and g) derived from the initial ee model fit. The excellent agreement between the experimental and predicted data for the final product enantioselectivity thus provides an independent corroboration of the proposed mechanistic hypothesis that the reaction proceeds through chiral species of relative concentrations and activities as described by the ML_2 model of the initial enantioselectivity data.

The reaction simulation also highlights special implications of nonlinear effects in stoichiometric reactions due to the fact that the chiral auxiliary is consumed in the reaction. When only 1 equiv of a chiral reagent is used in a reaction with 1:1 stoichiometry, the final product enantioselectivity at 100% conversion will necessarily be a linear reflection of the enantiomeric excess of the chiral auxiliary.[5b] This is illustrated in Figure 3a for the simulation of the reaction for the case of $ee_{aux} = 0.5$.[13] Asymmetric amplification is observed at lower conversions where the concentration of the more active and selective *dd* species is higher, as shown in Figure 3b; however, as this species is consumed, conversion to the product will ultimately be completed by the less active *meso* fraction. This is reflected in the reaction rate as well as in the product ee: the final 40% conversion proceeded at a rate 10 times slower than the first 60%. While the ratio of the homochiral species [*dd*]:[*ll*] remains constant over the course of the reaction, the lower reactivity of the *dl* species means that the reaction is, in effect, a kinetic resolution of the *dl* species. Therefore a single value for the parameter K, which describes the relationship between *meso* and homochiral species, is not physically meaningful for the description of a stoichiometric reaction where the relative concentrations of the species change with reaction time.

This inexorable erosion of product enantioselectivity may be combatted by judicious selection of an excess amount of the chiral reagent. An ML_2 model fit of initial enantioselectivity data allows determination of the level of excess chiral reagent required to minimize the contribution from the less active *meso* complex, which will depend on the parameters K and g as well as the value of ee_{aux}. For example, addition of a 50% excess of the chiral reagent for the reaction shown in Figure 3 will provide the correct stoichiometry to obtain a high yield by using primarily the enantioselective *dd* reagent, and for this example

(12) The datum point $ee_{aux} = 0.7$ was used to fix the endpoint sampling time for the reaction simulations for the other ee_{aux} data points as described in the Experimental section.

(13) The reactions described in ref 9c and simulated in Figure 1 were carried out with 1 equiv of chiral reagent but did not proceed to 100% conversion.

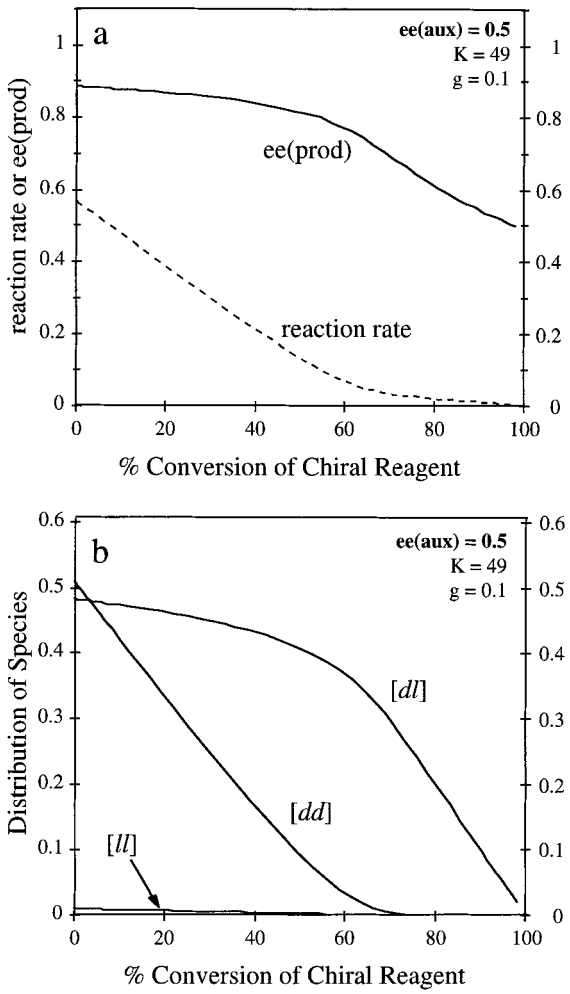

Figure 3. Simulation of the reaction shown in eq 1 and Scheme 1 with use of 1 equiv of Ipc_2BCl at $ee_{aux} = 0.5$. (a) Product enantioselectivity and reaction rate as a function of conversion of the chiral auxiliary. (b) Change in the relative concentrations of the *dd*, *ll*, and *dl* species as a function of conversion of the chiral auxiliary.

the required excess will be lower at higher values of ee_{aux}. In a case where the *meso* species is completely inactive, while no erosion of enantioselectivity will be observed, a properly chosen excess amount of chiral reagent will nevertheless be required to achieve full conversion of the substrate.

Extension to Catalytic Systems. In the case of catalytic reactions which follow an ML_n model, the effect on product enantioselectivity noted above for stoichiometric reactions should not occur, because the completion of repeated turnovers regenerating the chiral catalytic species can result in a sustained asymmetric amplification. In this case, storing the minor enantiomer as less active *meso* or heterochiral compounds can be an effective in-situ method of preparing an enantiopure chiral catalyst. Although overall productivity in the catalytic reaction may be adversely affected,[7] product enantioselectivity should not be a function of conversion in this case. Observation of a conversion-dependent enantioselectivity may thus imply a kinetically more complicated mechanism than that described by the ML_n models. Such conversion dependence,[6c,h,i] as well as seemingly inexplicable effects of changes in variables such as temperature,[6f] solvent,[6e,l] or catalyst/ligand concentration,[6c,i,l] have been reported, but seldom in sufficient detail to permit meaningful kinetic modeling. Provided that sufficient data are available, reaction simulations based on a model fit to initial ee data could help to rationalize the observed effects in these cases. Examples from the literature where this kinetic approach might explain deviations from the assumptions of the ML_n models are discussed below.

Bolm and co-workers[6c] reported asymmetric amplification in the conjugate addition of dialkylzinc compounds to chalcones catalyzed by Ni complexes with chiral pyridine ligands. They noted a strong conversion dependence of enantioselectivity which was also confirmed by Feringa and co-workers[6i] for similar systems. Bolm attributed the conversion dependence of enantioselectivity to the formation of more stable but less selective catalyst species over the course of the reaction. Although the final enantioselectivity data give a reasonable fit to an ML_2 model,[4a] mechanistic interpretation based on these model parameters may not be meaningful since the model assumes that no changes in the catalytic species occur during the reaction. Indeed, initial enantioselectivity data suggest that the asymmetric amplification may be even more pronounced than is apparent from the final product enantioselectivity data: a catalyst with 19% enantiopurity initially gave 87% product enantioselectivity (the same initial product selectivity as a 90% enantiopure catalyst), whereas at full conversion, the asymmetric amplification decreased to 52% product ee. The initial ee data are reminiscent of the extreme asymmetric amplification observed in the enantioselective addition of dialkylzinc to aldehydes catalyzed by chiral amino alcohols studied extensively by Noyori and co-workers,[6b,k] where an inactive *meso* complex was the most dominant species at lower catalyst enantiopurity. However, the ML_2 model fit to the final product enantioselectivity data in the case of Bolm and co-workers' data would assign an activity to the *meso* species which is at least 10 times greater than that which may be estimated from the two reported initial enantioselectivity data points. The initial enantioselectivity data provide a more realistic description of the pristine catalyst system and could be used as the starting point to model the proposed changes in the catalytic species over the course of the reaction.

Another assumption of the ML_n models is that reactions carried out with different catalytic species in a nonenantiopure mixture exhibit the same substrate concentration dependence. It may easily be imagined, however, that interactions between two enantiomeric catalysts which result in the formation of new diastereomeric species might result in changes in substrate binding constants such that the observed reaction rate law for a *meso* or heterochiral species may differ from that for the pure enantiomers. If different catalytic species in a nonenantiopure mixture of asymmetric catalysts exhibit different reaction rate laws and different intrinsic product enantioselectivities, the overall observed product enantioselectivity will vary with conversion in a manner amenable to the kinetic modeling approach described here.[14]

If the product of an asymmetric reaction inhibits or accelerates the rate of the enantioselective reaction, the ML_n models again become invalid for use with final product enantioselectivity data. An example of this is the case of asymmetric catalytic autoinduction or autocatalysis,[15] where reactions carried out using catalysts of low initial enantiopurity give reaction products

(14) Blackmond, D. G. In *Catalysis of Organic Reactions*; Herkes, F., Ed.; Marcel Dekker: New York, 1998; Vol. 36, pp 455−465.

(15) (a) Frank, F. C. *Biochim. Biophys. Acta* **1953**, *11*, 459. (b) Wynberg, H. *J. Macromol. Sci-Chem.* **1989**, *A26*, 1033. (c) Soai, K.; Niwa, S.; Hori, H. *J. Chem. Soc., Chem. Commun.* **1990**, 982. (d) Danda, J.; Nishikawa, H.; Otaka, K. *J. Org. Chem.* **1991**, *56*, 6740. (e) ShengJian, L.; Yaozhong, J.; Aiqiao, M.; Guishu, Y. *J. Chem. Soc., Perkin Trans. 1*, **1993**, 885. (f) Soai, K.; Shibata, T.; Morioka, H.; Choji, K. *Nature* **1995**, *378*, 767. (g) Shibata, T.; Morioka, H.; Hayase, T.; Choji, K.; Soai, K. *J. Am. Chem. Soc.* **1996**, *118*, 471.

of increasing enantioselectivity as conversion increases. For example, Soai[15f] showed that the autocatalytic formation of a chiral pyrimidyl alcohol in a reaction starting with the alcohol at 5% ee gave a product enantioselectivity of initially 55% and ultimately 90%.[16] In the simplest case of autocatalysis, the rate should depend on both the initial concentrations of catalyst species and the amount of product present in the mixture at any time. Reaction simulation based on initial enantioselectivity data could thus be used to provide corroboration in cases where an autocatalytic reaction mechanism is proposed.

Conclusions

The relationship between the enantiomeric excess of a reaction product and the enantiopurity of the catalyst or auxiliary used in the asymmetric reaction may provide a useful tool for mechanistic analysis. The examples given here show, however, that whenever two or more nonenantiomeric catalyst species compete in the same reaction mixture, the possiblity of a temporal (or conversion) dependence on enantioselectivity should not be excluded a priori. The manifestation of nonlinearity in a catalyst system is in most cases reported as a plot of the relationship between the final product enantioselectivity at the end of an asymmetric catalytic reaction and the enantiopurity of the catalyst that was added prior to the start of the reaction. Each data point on a plot of the relationship between the final product enantioselectivity and the enantiopurity of the catalyst or auxiliary may in fact represent a convolution of complex kinetic behavior over the course of the reaction. This paper demonstrates how initial enantioselectivity data may be useful in fixing the parameters at the starting point of the reaction to yield the information needed to formulate a description of the system as the reaction progresses. This work further suggests that experimental kinetic studies may aid in deconvoluting such complex behavior toward a fuller mechanistic understanding, and practical exploitation, of nonlinear behavior in asymmetric synthesis.

Experimental Section

Calculations concerning the reaction simulation which data from ref 9c are described. The initial enantioselectivity data points in Figure 1a were fit to the equation for $ee_{prod,i}$ given in Scheme 1 for an ML_2 model using the Excel Solver program (solid line in Figure 1a). The values of $[dd]_i$, $[ll]_i$, and $[dl]_i$ at each value of ee_{aux} (Figure 2) were used in mathematical simulations of the rates for reactions with chiral reagents having ee_{aux} values from 0 to 0.7 (eqs 3−9). The reaction is assumed to be first order in the chiral species, and the total reaction rate is the sum of the individual reactions. The reaction stoichiometry is assumed to be one to one between the chiral species and the product. Since the experimental value of the rate constant k_{dd} is not known (only its value relative to k_{dl} is given by the ML_2 model), the reaction was simulated by setting $k_{dd} = 1$ and using arbitrary units for time. The reaction simulations were carried out to an identical fixed time, representing the experimental endpoint of $t = 18$ h when the $ee_{prod,f}$ data were obtained, for each of eight cases of ee_{aux} (a simulation of reaction rate for the racemic case was carried out even though it gives a product enantioselectivity of zero). The experimental $ee_{prod,f}$ for the datum point $ee_{aux} = 0.7$ was used to fix the simulation time corresponding to the endpoint sampling time for the reaction, and this time was used as the endpoint in simulations for the other ee_{aux} data points shown in Figure 1b. Thus six of the simulated final product enantioselectivity data points (0.1, 0.2, 0.3, 0.4, 0.5, and 0.6) are independent of the experimental final product enantioselectivity data.

$$r_{total} = r_{dd} + r_{ll} + r_{dl} \tag{3}$$

$$r_{dd} = \frac{d[dd]}{dt} = k_{dd}[dd] \tag{4}$$

$$r_{ll} = \frac{d[ll]}{dt} = k_{dd}[ll] \tag{5}$$

$$r_{dl} = \frac{d[dl]}{dt} = g^{*}k_{dd}[dl] \tag{6}$$

$$[dd] = [dd]_i \exp(-k_{dd}t) \tag{7}$$

$$[ll] = [ll]_i \exp(-k_{dd}t) \tag{8}$$

$$[dl] = [dl]_i \exp(-g^{*}k_{dd}t) \tag{9}$$

Acknowledgment. Funding from the Max-Planck-Gesellschaft and from Pfizer, Inc. Central Research are gratefully acknowledged. Stimulating discussions with Prof. J. R. Sowa, Jr. (Seton Hall University), Prof. H. B. Kagan (Université Paris-Sud), Prof. E. N. Jacobsen and his group (Harvard University), and Dr. A. B. E. Minidis (formerly MPI, currently University of Stockholm) are gratefully acknowledged.

Supporting Information Available: Derivation of eq 2 (2 pages, print/PDF). See any current masthead page for ordering information and Web access instructions.

JA982448U

(16) The initial datum point in ref 15f was acquired at over 40% conversion of substrate, and hence probably does not strictly represent an initial value for the product enantioselectivity.